

A new modified WINDMI jerk system with exponential and sinusoidal nonlinearities, its bifurcation analysis, multistability, circuit simulation and synchronization design

Mohamad Afendee MOHAMED , Sundarapandian VAIDYANATHAN , Fareh HANNACHI ,
Aceng SAMBAS  and P. DARWIN 

In this work, a new 3-D modified WINDMI chaotic jerk system with exponential and sinusoidal nonlinearities is presented and its dynamical behaviours and properties are investigated. Firstly, some properties of the system are studied such as equilibrium points and their stability, Lyapunov exponents and Kaplan-Yorke dimension. Also, we study the new jerk system dynamics using numerical simulations and analyses, including phase portraits, Lyapunov exponent spectrum, bifurcation diagram and Poincaré map, 0-1 test. Next, we exhibit that the new 3-D chaotic modified WINDMI jerk system has multistability with coexisting chaotic attractors. Moreover, we design an electronic circuit using MultiSim 14.1 for real implementation of the modified WINDMI chaotic jerk system. Finally, we design an active synchronization scheme for the complete synchronization of the modified WINDMI chaotic jerk systems via backstepping control.

Key words: chaos, jerk systems, chaotic systems, Lyapunov exponents, bifurcation, multistability, circuit simulation, backstepping control

Copyright © 2023. The Author(s). This is an open-access article distributed under the terms of the Creative Commons Attribution-NonCommercial-NoDerivatives License (CC BY-NC-ND 4.0 <https://creativecommons.org/licenses/by-nc-nd/4.0/>), which permits use, distribution, and reproduction in any medium, provided that the article is properly cited, the use is non-commercial, and no modifications or adaptations are made

M.A. Mohamed (e-mail: mafendee@unisza.edu.my) is with Faculty of Information and Computing, Universiti Sultan Zainal Abidin, Terengganu, Malaysia.

S. Vaidyanathan (corresponding author, e-mail: sundarvtu@gmail.com) is with Centre for Control Systems, Vel Tech University, 400 Feet Outer Ring Road, Avadi, Chennai-600062 Tamil Nadu, India and Faculty of Information and Computing, Universiti Sultan Zainal Abidin Terengganu, Malaysia.

F. Hannachi (e-mail: fareh.hannachi@univ-tebessa.dz) is with Larbi Tebessi University – Tebessi route de constantine, 12022, Tebessa, Algeria.

A. Sambas (e-mails: acengsambas@unisza.edu.my, acengs@umtas.ac.id) is with Faculty of Informatics and Computing, Universiti Sultan Zainal Abidin Gong Badak, 21300, Terengganu, Malaysia and Department of Mechanical Engineering, Universitas Muhammadiyah Tasikmalaya, Jawa Barat 46196, Indonesia.

P. Darwin (e-mail: darwin009@gmail.com) is with Department of Information Technology, Tagore Engineering College, Rathinamangalam, Chennai - 600127, Tamil Nadu, India.

Received 11.06.2023. Revised 9.08.2023.

1. Introduction

In view of their complexity and unpredictability, chaotic dynamical systems are applicable in several scientific and engineering areas such as machine learning [1, 2], image encryption [3–5], FPGA design [6, 7], memristors [8, 9], chemical reactions [10], etc.

Autonomous chaotic jerk systems are characterized by third order differential equations of the form

$$\ddot{p} = g(p, \dot{p}, \ddot{p}) \quad (1)$$

which have Lyapunov exponents having the signs (+, 0, –). These chaotic systems are *conservative* when the sum of their Lyapunov exponents is zero and *dissipative* when the sum of their Lyapunov exponents is negative [11].

It is convenient to represent the autonomous jerk ODE (1) in the following representation of an autonomous system of first order differential equations.

$$\begin{aligned} \dot{p} &= q, \\ \dot{q} &= r, \\ \dot{r} &= g(p, q, r), \end{aligned} \quad (2)$$

where $p(t)$, $q(t)$ and $r(t)$ are the three states of the autonomous jerk system (2). Chaotic jerk systems arise in mechanical engineering and the state variables $p(t)$, $q(t)$ and $r(t)$ can be given a physical interpretation as displacement, velocity and acceleration for a moving body.

Many research studies have been made on chaotic jerk systems in the recent years [12–15]. Li and Zeng [12] described a multi-scroll attractor with multistability behavior in a 3-D jerk system with a sinusoidal nonlinearity. Dongmo *et al.* [13] reported the FPGA implementation of an autonomous Josephson junction jerk system with multistability. Ramadoss *et al.* [14] studied the circuit realization of a chaotic jerk system with septic nonlinearity. Lai and Lai [15] found a memristive chaotic system with multistability and offset shooting behavior and described its hardware implementation.

A WINDMI Chaotic System stands for the Wind-Magnetosphere-Ionosphere system which represents the energy influx from the solar wind-magnetosphere-ionosphere system [16]. A mathematical model of WINDMI chaotic system with an exponential nonlinearity was proposed by Sprott [17]. In this research work, we add a sinusoidal nonlinearity to the WINDMI chaotic jerk system and obtain a new chaotic jerk system with more complexity.

We carry out a detailed bifurcation analysis of the new modified WINDMI chaotic jerk system with exponential and sinusoidal nonlinearities. It is well-known that bifurcation analysis of dynamical systems with respect to changes in the parameter values give an in-depth view of the qualitative nature of the underlying systems [18–20]. We also exhibit that the new modified WINDMI

chaotic jerk system has multistability with coexisting attractors. Multistability of a chaotic system refers to the coexistence of chaotic attractors for the same set of parameter values but different initial states [21–23].

Next, we design an electronic circuit via MultiSim 14.1 for the new modified WINDMI chaotic jerk system with exponential and sinusoidal nonlinearities. Circuit design for chaotic systems is useful for applications [24–26]. Finally, as a control application, we derive new results for the complete synchronization of a pair of new modified WINDMI chaotic jerk systems taken as the *master* and *slave* systems via backstepping control technique. Synchronization of chaotic systems has many applications in control engineering such as cryptosystems, secure communications, etc. [27–29]. The backstepping control technique is a simple recursive design procedure that associates the choice of the control Lyapunov function with the suitable design of a feedback controller [30, 31]. Backstepping control has many engineering applications [32, 33].

2. Description of the new chaotic jerk system

A WINDMI Chaotic System stands for the Wind-Magnetosphere-Ionosphere system which represents the energy influx from the solar wind-magnetosphere-ionosphere system. A mathematical model of WINDMI chaotic system was proposed by Sprott [17] as the following jerk dynamics:

$$\begin{aligned}\dot{x} &= y, \\ \dot{y} &= z, \\ \dot{z} &= -az - y + b - e^x,\end{aligned}\tag{3}$$

where x, y, z are the state variables and a, b, c are positive parameters.

It was shown by Sprott [17] that the WINDMI system (3) is chaotic for the parameter values taken as follows:

$$a = 0.7, \quad b = 2.5.\tag{4}$$

For the initial state $(x(0), y(0), z(0)) = (0.5, 0.2, 0.5)$ and $(a, b) = (0.7, 2.5)$, the Lyapunov exponents for the WINDMI system (3) were calculated for $T = 1E4$ seconds as follows:

$$L_1 = 0.0758, \quad L_2 = 0, \quad L_3 = -0.7758.\tag{5}$$

The Kaplan-Yorke dimension for the WINDMI chaotic system (3) is found as follows:

$$D_K = 2 + \frac{L_1 + L_2}{|L_3|} = 2.0977.\tag{6}$$

In this work, we obtain a modified WINDMI chaotic system by introducing a sinusoidal nonlinearity to the WINDMI chaotic system (3). Thus, we propose the following new jerk dynamics:

$$\begin{aligned}\dot{x} &= y, \\ \dot{y} &= z, \\ \dot{z} &= -az - y + b + c \sin(y) - e^x,\end{aligned}\tag{7}$$

where x, y, z are the state variables and a, b, c are positive parameters.

In this work, we shall establish that the modified WINDMI system (7) is chaotic for the parameter values taken as follows:

$$a = 0.7, \quad b = 2.5, \quad c = 0.2.\tag{8}$$

For the initial state $(x(0), y(0), z(0)) = (0.5, 0.2, 0.5)$ and $(a, b) = (0.7, 2.5, 0.2)$ the Lyapunov exponents for the modified WIDMI system (7) were calculated for $T = 1E4$ seconds as follows:

$$L_1 = 0.0993, \quad L_2 = 0, \quad L_3 = -0.7993.\tag{9}$$

The Kaplan-Yorke dimension for the modified WINDMI chaotic system (7) is found as follows:

$$D_K = 2 + \frac{L_1 + L_2}{|L_3|} = 2.1242.\tag{10}$$

The values of the MLE and D_{KL} for the modified WINDMI system (7) are greater than the values of the MLE and D_K for the WINDMI chaotic system (3) respectively, exhibiting that the modified WINDMI chaotic system (7) has more complexity than the WINDMI chaotic system (3).

Clearly, the modified WINDMI system (7) has a unique equilibrium point given by:

$$x = \ln(b), \quad y = 0, \quad z = 0.\tag{11}$$

For the chaotic case (8), the unique equilibrium point of the system (7) is obtained as

$$x = 0.916290, \quad y = 0, \quad z = 0.\tag{12}$$

The eigenvalues of the Jacobian matrix of the new modified WINDMI system (7) at the equilibrium point: $E_0 = (0.916290, 0, 0)$ are found as follows::

$$\begin{aligned}\lambda_1 &= -1.4017, & \lambda_2 &= 0.35085 + 1.2886i, \\ \lambda_3 &= 0.35085 - 1.2886i.\end{aligned}\tag{13}$$

Hence, E_0 is a saddle-focus point and it is unstable for the new chaotic jerk system (7).

Figure 1 portrays the 2-D and 3-D plots of the chaotic attractor of the new modified WINDMI chaotic jerk system (7) for $(x(0), y(0), z(0)) = (0.5, 0.2, 0.5)$ and $(a, b, c) = (0.7, 2.5, 0.2)$.

Figure 2 shows the plots of the Poincaré section of the new modified WINDMI chaotic jerk system (7) in different planes.

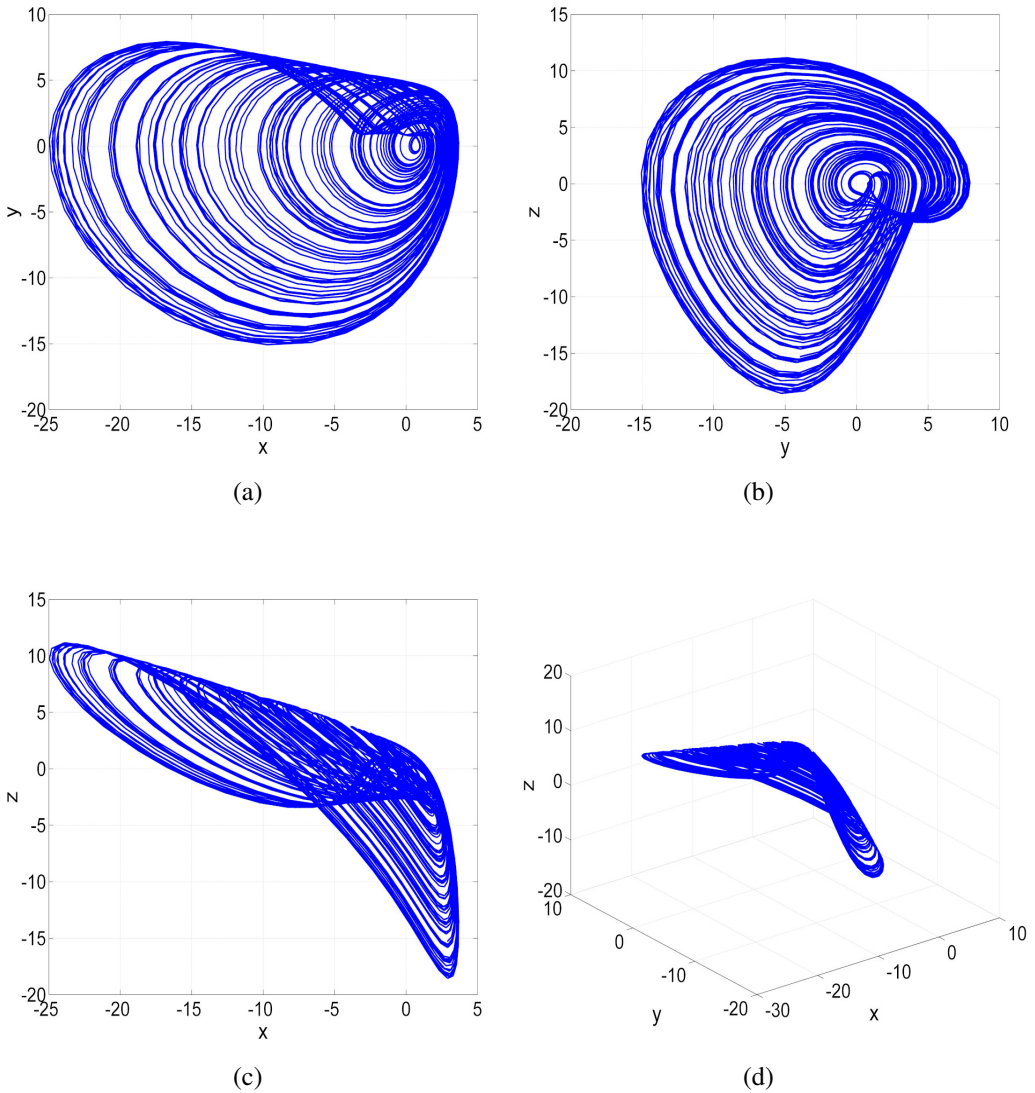


Figure 1: 2-D and 3-D plots of the chaotic attractor of the new modified WINDMI jerk system (7) for $(x(0), y(0), z(0)) = (0.5, 0.2, 0.5)$ and $(a, b, c) = (0.7, 2.5, 0.2)$

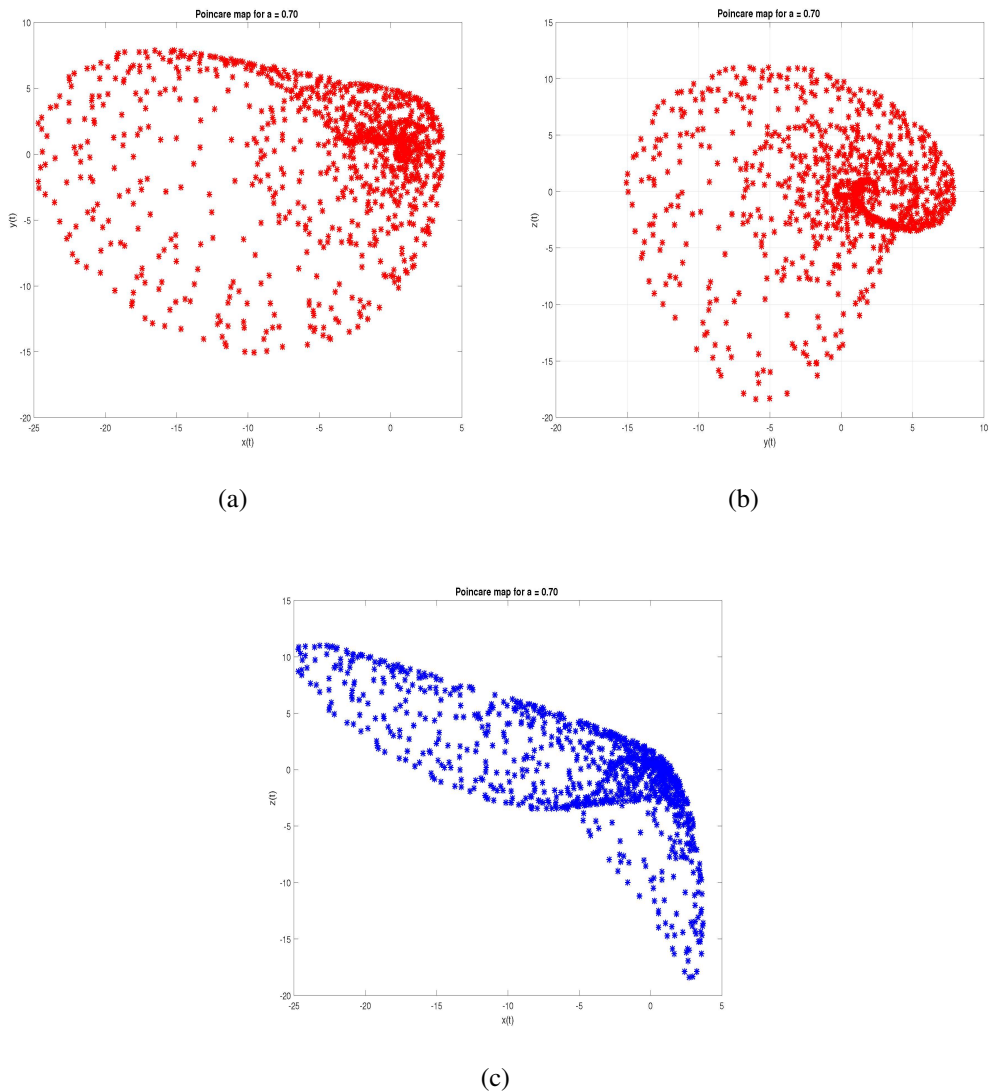


Figure 2: Plots of the Poincaré section of the new modified WINDMI chaotic jerk system (7) in different planes for $a = 0.7$

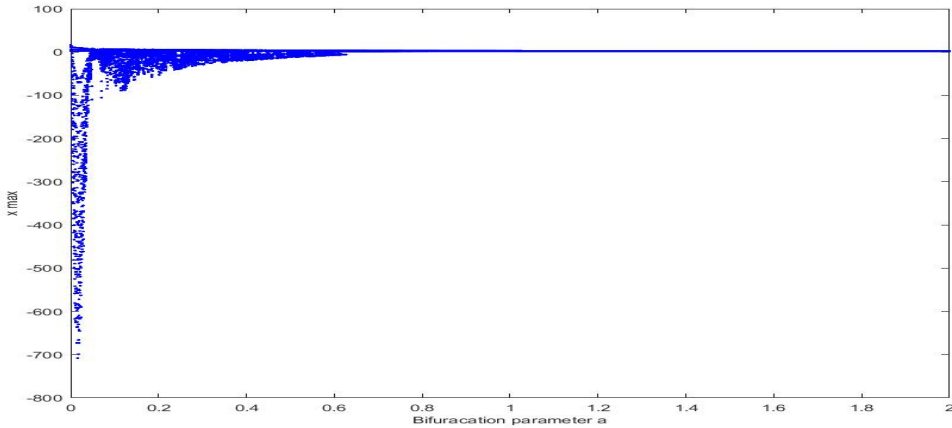
3. Bifurcation analysis of the new modified WINDMI jerk system

3.1. Changes with respect to the parameter a

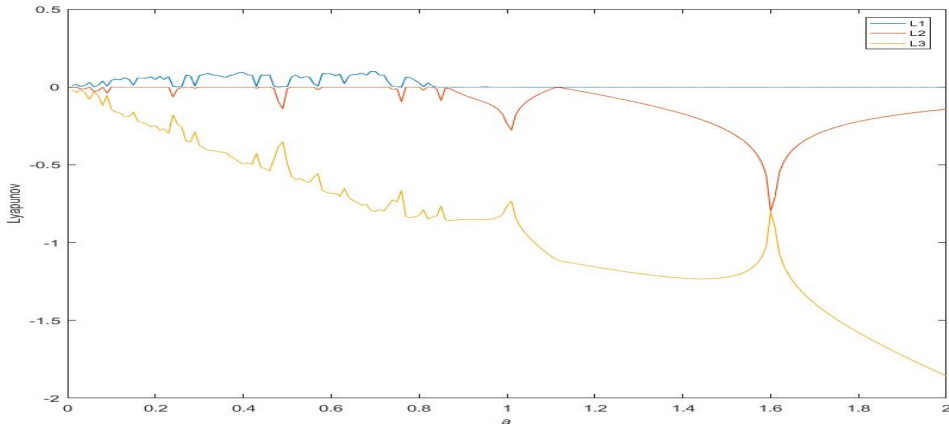
We fix the values of b and c as $b = 2.5$ and $c = 0.2$.

When $a \in [0, 2]$, the behavior of the new modified WINDMI jerk system (7) is either chaotic or periodic.

Figure 3 shows the bifurcation diagram and Lyapunov exponents of the new modified WINDMI jerk system (7) when a varies in the interval $[0, 2]$.



(a) Bifurcation Diagram



(b) Lyapunov Exponents

Figure 3: Bifurcation diagram and Lyapunov exponents of the new modified WINDMI jerk system (7) when $b = 2.5$, $c = 0.2$ and $a \in [0, 2]$

We divide the interval $[0, 2]$ into two subsets A and B , which are defined as follows:

$$A = (0, 0.06) \cup (0.06, 0.81) \cup (0.81, 0.85), \quad (14)$$

$$B = [0.24, 0.26] \cup [0.85, 2] \cup \{0.06\}. \quad (15)$$

When $a \in A$, we can see from Figure 3 that the Lyapunov exponents of the new modified WINDMI jerk system (7) has signs $(+, 0, -)$. Thus, the new modified WINDMI jerk system (7) is chaotic for $a \in A$.

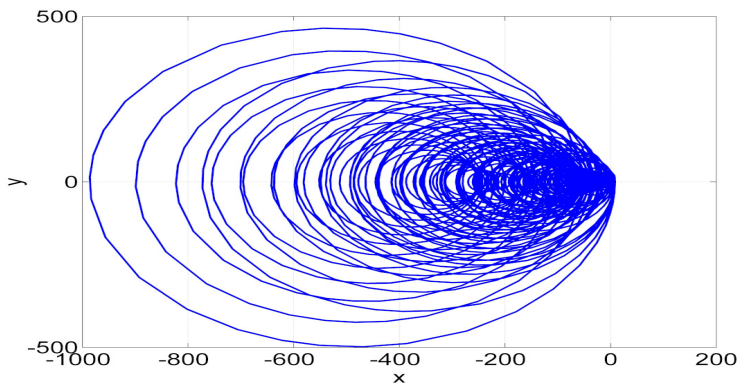
When $a = 0.05$, the Lyapunov exponents of the new modified WINDMI jerk system (7) are obtained as

$$L_1 = 0.03028, \quad L_2 = 0, \quad L_3 = -0.08073. \quad (16)$$

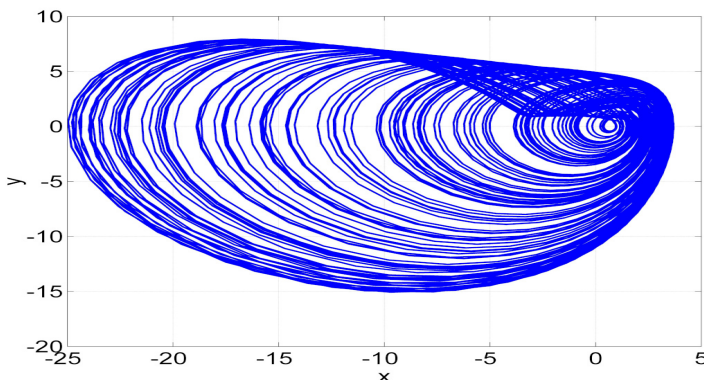
When $a = 0.7$, the Lyapunov exponents of the new modified WINDMI jerk system (7) are obtained as

$$L_1 = 0.1004, \quad L_2 = 0, \quad L_3 = -0.8005. \quad (17)$$

Figure 4 shows the chaotic attractors of the new modified WINDMI jerk system (7) for $b = 2.5$, $c = 0.2$ and different values of $a \in A$.



(a) $a = 0.05$



(b) $a = 0.7$

Figure 4: Chaotic attractors of the new modified WINDMI jerk system (7) for $b = 2.5$, $c = 0.2$ and different values of $a \in A$

When $a \in B$, we can see from Figure 3 that the Lyapunov exponents of the new modified WINDMI jerk system (7) has signs $(0, -, -)$. Thus, the new modified WINDMI jerk system (7) is periodic for $a \in B$.

When $a = 0.25$, the Lyapunov exponents of the new modified WINDMI jerk system (7) are obtained as

$$L_1 = 0, \quad L_2 = -0.01243, \quad L_3 = -0.2382. \quad (18)$$

When $a = 0.85$, the Lyapunov exponents of the new modified WINDMI jerk system (7) are obtained as

$$L_1 = 0, \quad L_2 = -0.08632, \quad L_3 = -0.7638. \quad (19)$$

When $a = 0.9$, the Lyapunov exponents of the new modified WINDMI jerk system (7) are obtained as

$$L_1 = 0, \quad L_2 = -0.04905, \quad L_3 = -0.8512. \quad (20)$$

Figure 5 shows the periodic attractors of the new modified WINDMI jerk system (7) for $b = 2.5, c = 0.2$ and different values of $a \in B$.

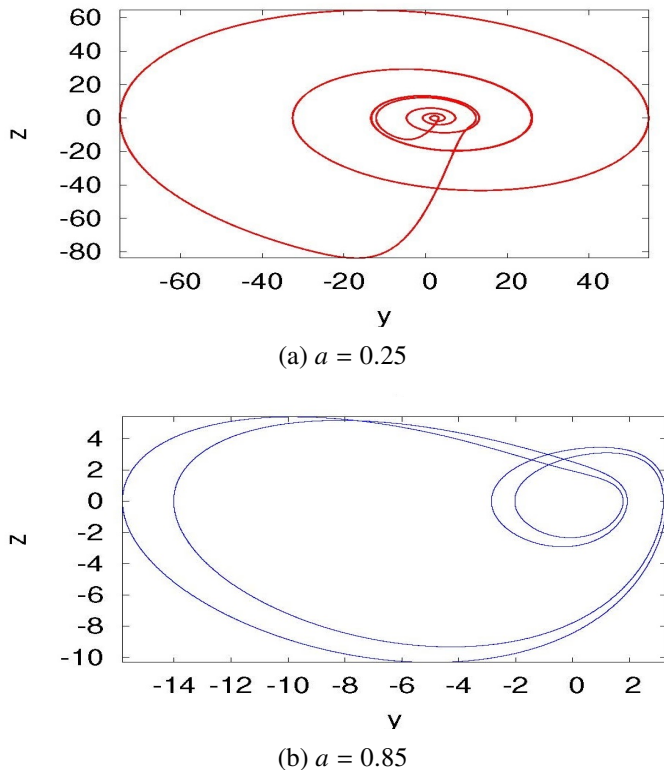


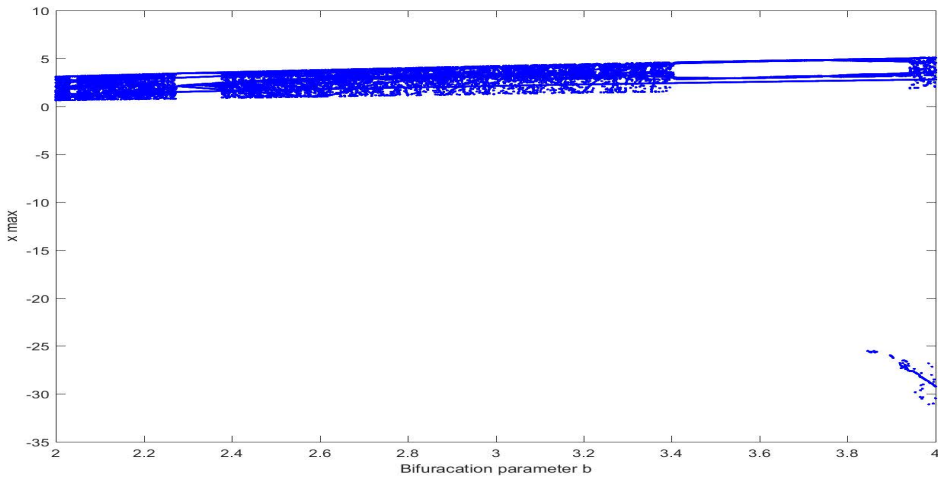
Figure 5: Periodic attractors of the new modified WINDMI jerk system (7) for $b = 2.5, c = 0.2$ and different values of $a \in B$

3.2. Changes with respect to the parameter b

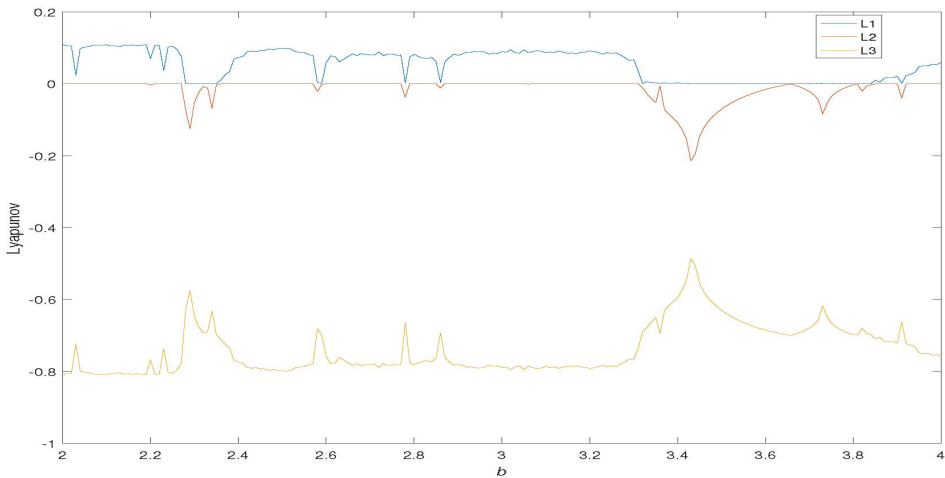
We fix the values of a and c as $a = 0.7$ and $c = 0.2$.

When $b \in [2, 4]$, the behavior of the new modified WINDMI jerk system (7) is either chaotic or periodic.

Figure 6 shows the bifurcation diagram and Lyapunov exponents of the new modified WINDMI jerk system (7) when b varies in the interval $[2, 4]$.



(a) Bifurcation Diagram



(b) Lyapunov Exponents

Figure 6: Bifurcation diagram and Lyapunov exponents of the new modified WINDMI jerk system (7) when $a = 0.7$, $c = 0.2$ and $b \in [2, 4]$

We divide the interval $[2, 4]$ into two subsets A and B , which are defined as follows:

$$A = [2, 2.28) \cup (2.35, 3.32) \cup (3.32, 3.44) \cup (3.84, 4), \quad (21)$$

$$B = [2.28, 2.35] \cup [3.44, 3.84] \cup \{3.32\}. \quad (22)$$

When $b \in A$, we can see from Figure 6 that the Lyapunov exponents of the new modified WINDMI jerk system (7) has signs $(+, 0, -)$. Thus, the new modified WINDMI jerk system (7) is chaotic for $b \in A$.

When $b = 2.1$, the Lyapunov exponents of the new modified WINDMI jerk system (7) are obtained as

$$L_1 = 0.1082, \quad L_2 = 0, \quad L_3 = -0.8085. \quad (23)$$

When $b = 2.8$, the Lyapunov exponents of the new modified WINDMI jerk system (7) are obtained as

$$L_1 = 0.01873, \quad L_2 = 0, \quad L_3 = -0.7818. \quad (24)$$

When $b = 3.95$, the Lyapunov exponents of the new modified WINDMI jerk system (7) are obtained as

$$L_1 = 0.04806, \quad L_2 = 0, \quad L_3 = -0.748. \quad (25)$$

Figure 7 shows the chaotic attractors of the new modified WINDMI jerk system (7) for $a = 0.7$, $c = 0.2$ and different values of $b \in A$.

When $b \in B$, we can see from Figure 6 that the Lyapunov exponents of the new modified WINDMI jerk system (7) has signs $(0, -, -)$. Thus, the new modified WINDMI jerk system (7) is periodic for $b \in B$.

When $b = 2.3$, the Lyapunov exponents of the new modified WINDMI jerk system (7) are obtained as

$$L_1 = 0, \quad L_2 = -0.05161, \quad L_3 = -0.6487. \quad (26)$$

When $b = 3.32$, the Lyapunov exponents of the new modified WINDMI jerk system (7) are obtained as

$$L_1 = 0, \quad L_2 = -0.010881, \quad L_3 = -0.6897. \quad (27)$$

When $b = 3.5$, the Lyapunov exponents of the new modified WINDMI jerk system (7) are obtained as

$$L_1 = 0, \quad L_2 = -0.07064, \quad L_3 = -0.6297 \quad (28)$$

Figure 8 shows the periodic attractors of the new modified WINDMI jerk system (7) for $a = 0.7$, $c = 0.2$ and different values of $b \in B$.

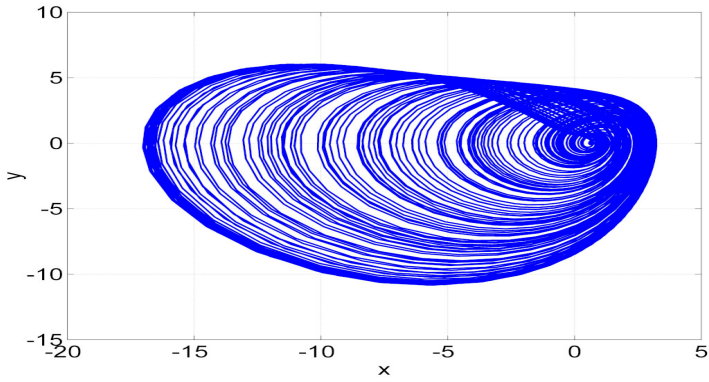
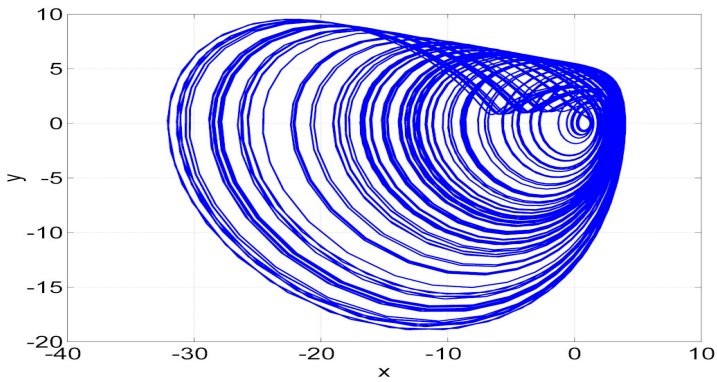
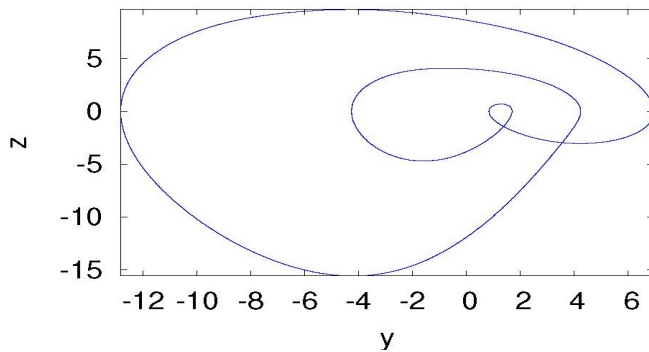
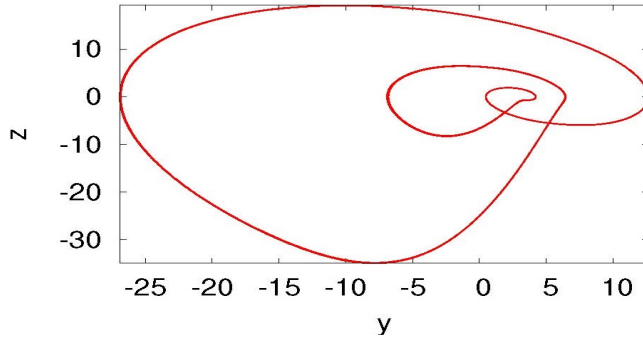
(a) $b = 2.1$ (b) $b = 2.8$

Figure 7: Chaotic attractors of the new modified WINDMI jerk system (7) for $a = 0.7$, $c = 0.2$ and different values of $b \in A$

(a) $b = 2.3$



(b) $b = 3.32$

Figure 8: Periodic attractors of the new modified WINDMI jerk system (7) for $a = 0.7$, $c = 0.2$ and different values of $b \in B$

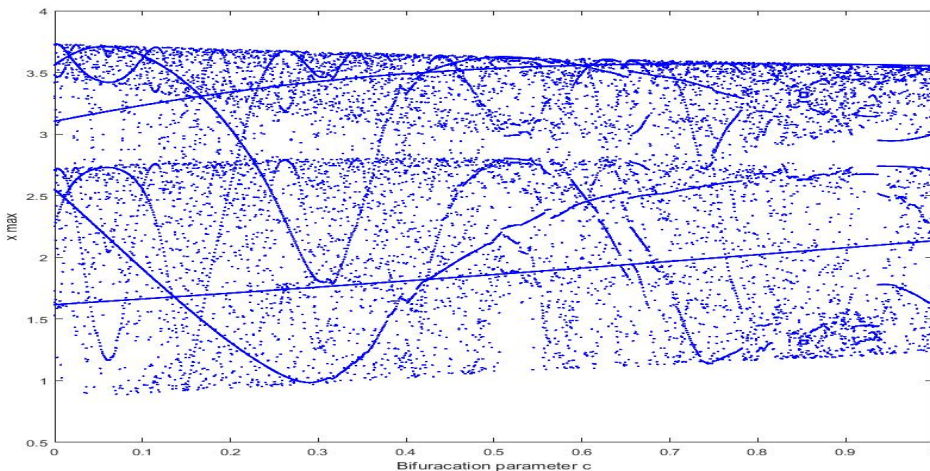
3.3. Changes with respect to the parameter c

We fix the values of a and b as $a = 0.7$ and $b = 2.5$.

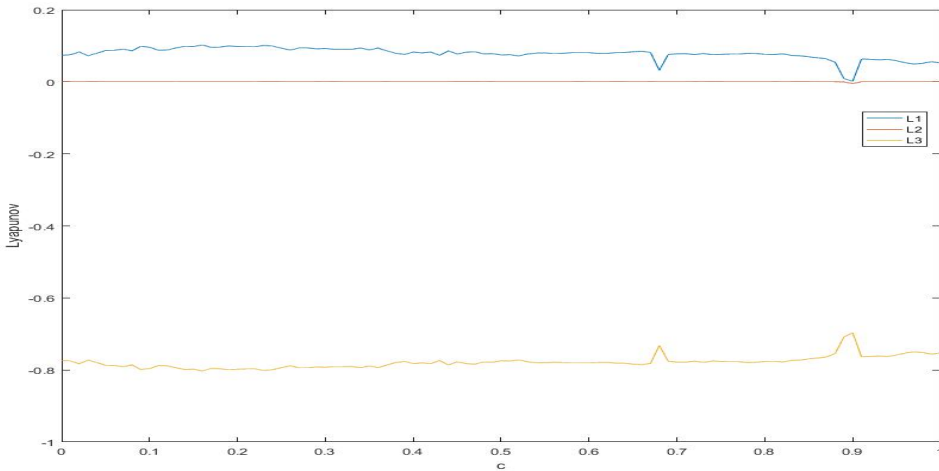
When $c \in [0, 1]$, the behavior of the new modified WINDMI jerk system (7) is either chaotic or periodic.

Figure 9 shows the bifurcation diagram and Lyapunov exponents of the new modified WINDMI jerk system (7) when c varies in the interval $[0, 1]$.

When $c \in [0, 1]$, we can see from Figure 6 that the Lyapunov exponents of the new modified WINDMI jerk system (7) has signs $(+, 0, -)$. Thus, the new modified WINDMI jerk system (7) is chaotic for $c \in [0, 1]$.



(a) Bifurcation Diagram



(b) Lyapunov Exponents

Figure 9: Bifurcation diagram and Lyapunov exponents of the new modified WINDMI jerk system (7) when $a = 0.7$, $b = 2.5$ and $c \in [0, 1]$

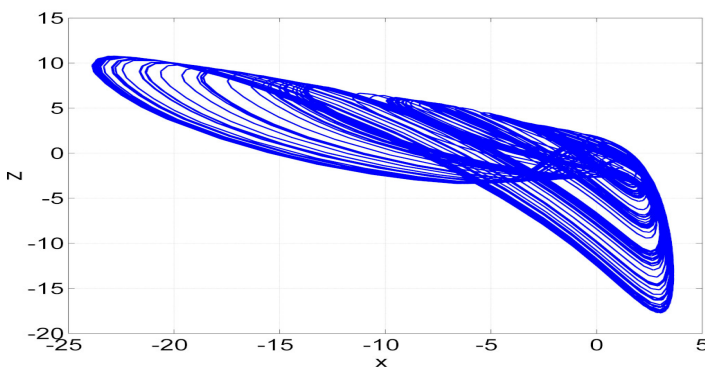
When $c = 0.5$, the Lyapunov exponents of the new modified WINDMI jerk system (7) are obtained as

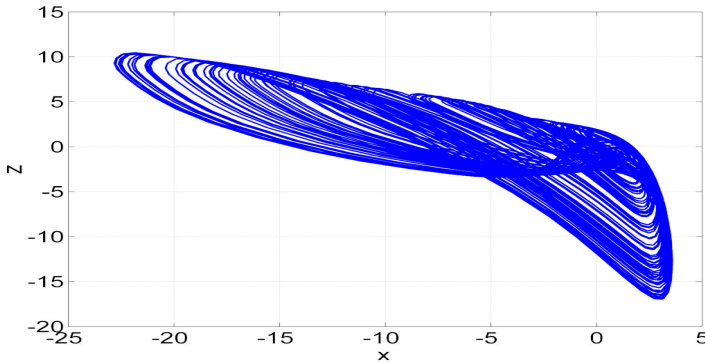
$$L_1 = 0.07448, \quad L_2 = 0, \quad L_3 = -0.7745. \quad (29)$$

When $c = 0.8$, the Lyapunov exponents of the new modified WINDMI jerk system (7) are obtained as

$$L_1 = 0.07626, \quad L_2 = 0, \quad L_3 = -0.7762. \quad (30)$$

Figure 10 shows the chaotic attractors of the new modified WINDMI jerk system (7) for $a = 0.7$, $b = 2.5$ and different values of $c \in [0, 1]$.

(a) $c = 0.5$



(b) $c = 0.8$

Figure 10: Chaotic attractors of the new modified WINDMI jerk system (7) for $a = 0.7$, $b = 2.5$ and different values of $c \in [0, 1]$

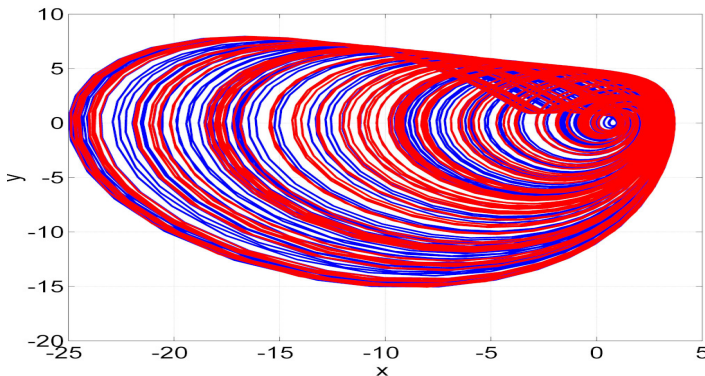
3.4. Multistability in the new 3-D chaotic jerk

Multistability refers to a special property of a chaotic dynamical system which stands for the coexistence of chaotic attractors for the same parameters but various values of the initial states.

For the new modified WINDMI jerk system (7), we choose the system parameters as in the chaotic case, viz. $a = 0.7$, $b = 2.5$ and $c = 0.2$.

We choose two initial states as $X_0 = (1, 0, -1)$ (blue orbit) and $Y_0 = (-1, -1, 1)$ (red orbit).

Figure 11 shows the multistability and coexistence of two chaotic attractors of the new modified WINDMI jerk system (7).



(a)

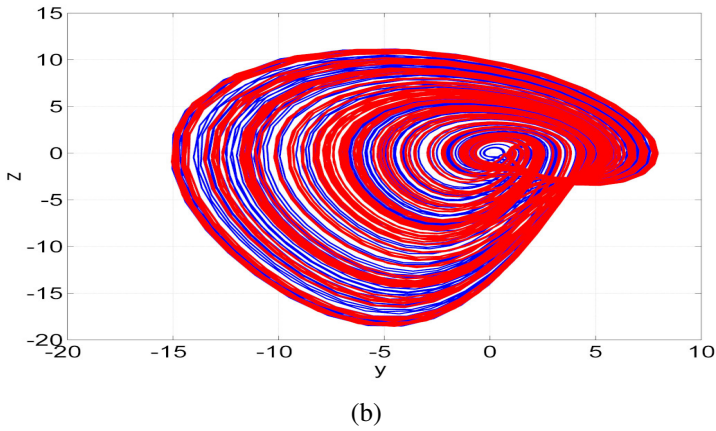


Figure 11: Multistability and coexistence of two chaotic attractors of the new modified WINDMI jerk system (7) where $a = 0.7$, $b = 2.5$ and $c = 0.2$. The initial states are chosen as $X_0 = (1, 0, -1)$ (blue orbit) and $Y_0 = (-1, -1, 1)$ (red orbit)

4. Complete synchronization of the new 3-D modified WINDMI chaotic jerk systems

Since the jerk systems have a special structure, we use the backstepping control technique [11] in order to achieve complete synchronization between the master and slave chaotic jerk systems.

For the synchronization design, we consider the master and slave modified WINDMI jerk systems, which are described as follows:

$$\begin{aligned} \dot{x}_m &= y_m, \\ \dot{y}_m &= z_m, \\ \dot{z}_m &= -az_m - y_m + b + c \sin(y_m) - e^{x_m}, \end{aligned} \quad (31)$$

$$\begin{aligned} \dot{x}_s &= y_s, \\ \dot{y}_s &= z_s, \\ \dot{z}_s &= -az_s - y_s + b + c \sin(y_s) - e^{x_s} + U. \end{aligned} \quad (32)$$

In Eq. (32), U is an active backstepping control to be found.

We define the complete synchronization error between the modified WINDMI jerk systems as follows:

$$\begin{aligned} E_x &= x_s - x_m, \\ E_y &= y_s - y_m, \\ E_z &= z_s - z_m, \end{aligned} \quad (33)$$

The error dynamics is derived by means of the following equations:

$$\begin{aligned} \dot{E}_x &= E_y, \\ \dot{E}_y &= E_z, \\ \dot{E}_z &= -aE_z - E_y + c[\sin(y_s) - \sin(y_m)] - [e^{x_s} - e^{x_m}] + U. \end{aligned} \tag{34}$$

In this section, we shall establish the following main result.

Theorem 1 *The backstepping control law defined by the equation*

$$U = -3E_x - 4E_y - (3 - a)E_z - c[\sin(y_s) - \sin(y_m)] + [e^{x_s} - e^{x_m}] - \kappa\psi_z \tag{35}$$

with gain $\kappa > 0$ and $\psi_z = 2E_x + 2E_y + E_z$ globally and exponentially stabilizes the modified WINDMI chaotic jerk systems (31) and (32) for all initial states in \mathbb{R}^3 .

Proof. We begin with the Lyapunov function

$$Q_1(\psi_x) = \frac{1}{2} \psi_x^2, \tag{36}$$

where

$$\psi_x = E_x. \tag{37}$$

Then we get

$$\dot{Q}_1 = \psi_x \dot{\psi}_x = -\psi_x^2 + \psi_x (E_x + E_y). \tag{38}$$

Next, we define

$$\psi_y = E_x + E_y. \tag{39}$$

Then Eq. (38) reduces to

$$\dot{Q}_1 = -\psi_x^2 + \psi_x \psi_y. \tag{40}$$

Next, we define the candidate Lyapunov function

$$Q_2(\psi_x, \psi_y) = Q_1(\psi_x) + \frac{1}{2} \psi_y^2 = \frac{1}{2} \psi_x^2 + \frac{1}{2} \psi_y^2. \tag{41}$$

We find that

$$\dot{Q}_2 = -\psi_x^2 - \psi_y^2 + \psi_y (2E_x + 2E_y + E_z). \tag{42}$$

To simplify the notations, we set

$$\psi_z = 2E_x + 2E_y + E_z \tag{43}$$

Then Eq. (42) reduces to

$$\dot{Q}_2 = -\psi_x^2 - \psi_y^2 + \psi_y\psi_z. \quad (44)$$

As a final step of the backstepping control design, we consider the candidate Lyapunov function

$$Q(\psi_x, \psi_y, \psi_z) = Q_2(\phi_x, \phi_y) + \frac{1}{2}\psi_z^2. \quad (45)$$

It is easy to see that Q is a quadratic, positive definite function defined on \mathbb{R}^3 .

We also find that

$$Q(\psi_x, \psi_y, \psi_z) = \frac{1}{2}\psi_x^2 + \frac{1}{2}\psi_y^2 + \frac{1}{2}\psi_z^2. \quad (46)$$

A simple calculation yields the following:

$$\dot{Q} = -E_x^2 - E_y^2 - E_z^2 + \psi_z W, \quad (47)$$

where

$$W = \psi_y + \psi_z + \dot{\psi}_z. \quad (48)$$

A simple calculation shows that

$$W = 3E_x + 4E_y + (3 - a)E_z + c [\sin(y_s) - \sin(y_m)] - [e^{x_s} - e^{x_m}] + U. \quad (49)$$

Substituting the formula given in Eq. (35) for U into Eq. (48), we get

$$W = -\kappa\psi_z. \quad (50)$$

Combining (47) and (50), we get

$$\dot{Q} = -\psi_x^2 - \psi_y^2 - \psi_z^2(1 + \kappa). \quad (51)$$

Since $\kappa > 0$, we see that \dot{Q} is a quadratic and negative definite function defined on \mathbb{R}^3 .

By Lyapunov Stability Theory, we deduce that the error dynamics (34) is globally exponentially stable.

This completes the proof. \square

For MATLAB simulations, we pick the parameter values as in the chaotic situation, *viz.* $a = 0.7$, $b = 2.5$ and $c = 0.2$. We choose $\kappa = 20$.

For simulations, the initial condition of the master system (31) is assumed as follows:

$$x_m(0) = 8.1, \quad y_m(0) = 2.4, \quad z_m(0) = 7.3. \quad (52)$$

Also, the initial condition of the master system (32) is assumed as follows:

$$x_s(0) = 1.9, \quad y_s(0) = 6.7, \quad z_s(0) = 5.8. \quad (53)$$

Figure 12 shows the convergence of the synchronization error ($E_x(t)$, $E_y(t)$, $E_z(t)$) between the jerk systems (31) and (32).

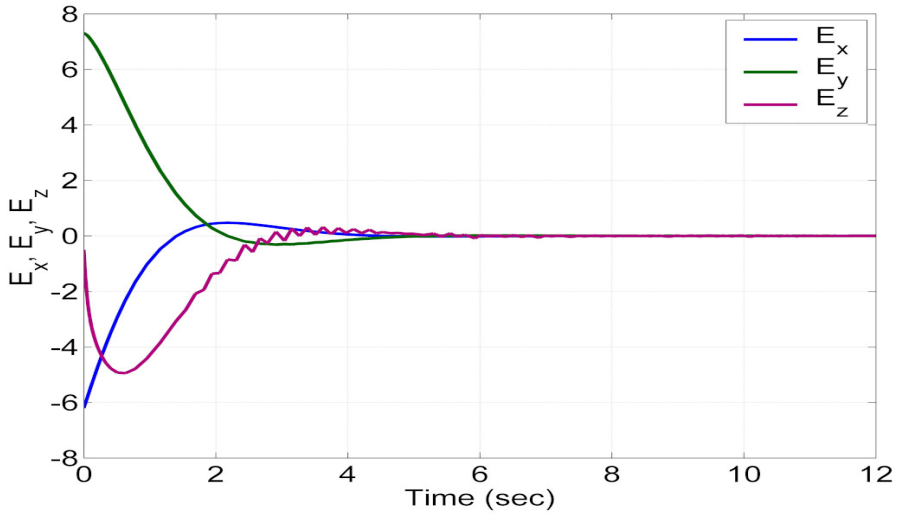


Figure 12: MATLAB plot showing the synchronization error (E_x, E_y, E_z) between the jerk systems (31) and (32)

5. Circuit simulation of the new 3-D modified WINDMI chaotic jerk system

In this section, the new 3-D modified WINDMI chaotic jerk system (7) is realized by the NI Multisim 14.1 platform. The electronic circuit design of the 3-D chaotic jerk system (7) is shown in Figure 13 in which TLO84ACN is selected as OPAMP and three diodes of type 1N4149. Applying the Kirchoff's laws, the circuit presented in Figure 13 is described by the following equations:

$$\begin{aligned} \dot{x} &= \frac{1}{R_1 C_1} y, \\ \dot{y} &= \frac{1}{R_2 C_2} z, \\ \dot{z} &= -\frac{1}{R_3 C_3} x - \frac{1}{R_5 C_3} y + \frac{v_1}{R_6 C_3} + \frac{1}{R_6 C_3} \sin(y) - \frac{1}{R_7 C_3} \exp(x). \end{aligned} \quad (54)$$

Here x, y, z correspond to the voltages on the integrators $U1C, U3C, U5C$, respectively. The values of components in the circuit are selected as:

$$R_1 = R_2 = R_5 = R_7 = 100 \text{ k}\Omega, \quad R_3 = 142.857 \text{ k}\Omega, \quad R_4 = 2500 \text{ k}\Omega, \quad (55)$$

$$R_i = 100 \text{ k}\Omega, \quad i = 8, 9, \dots, 19, \quad R_{20} = 20 \text{ k}\Omega, \quad R_{21} = 10 \text{ k}\Omega, \quad (56)$$

and

$$C_1 = C_2 = C_3 = 1 \text{ nF}. \quad (57)$$

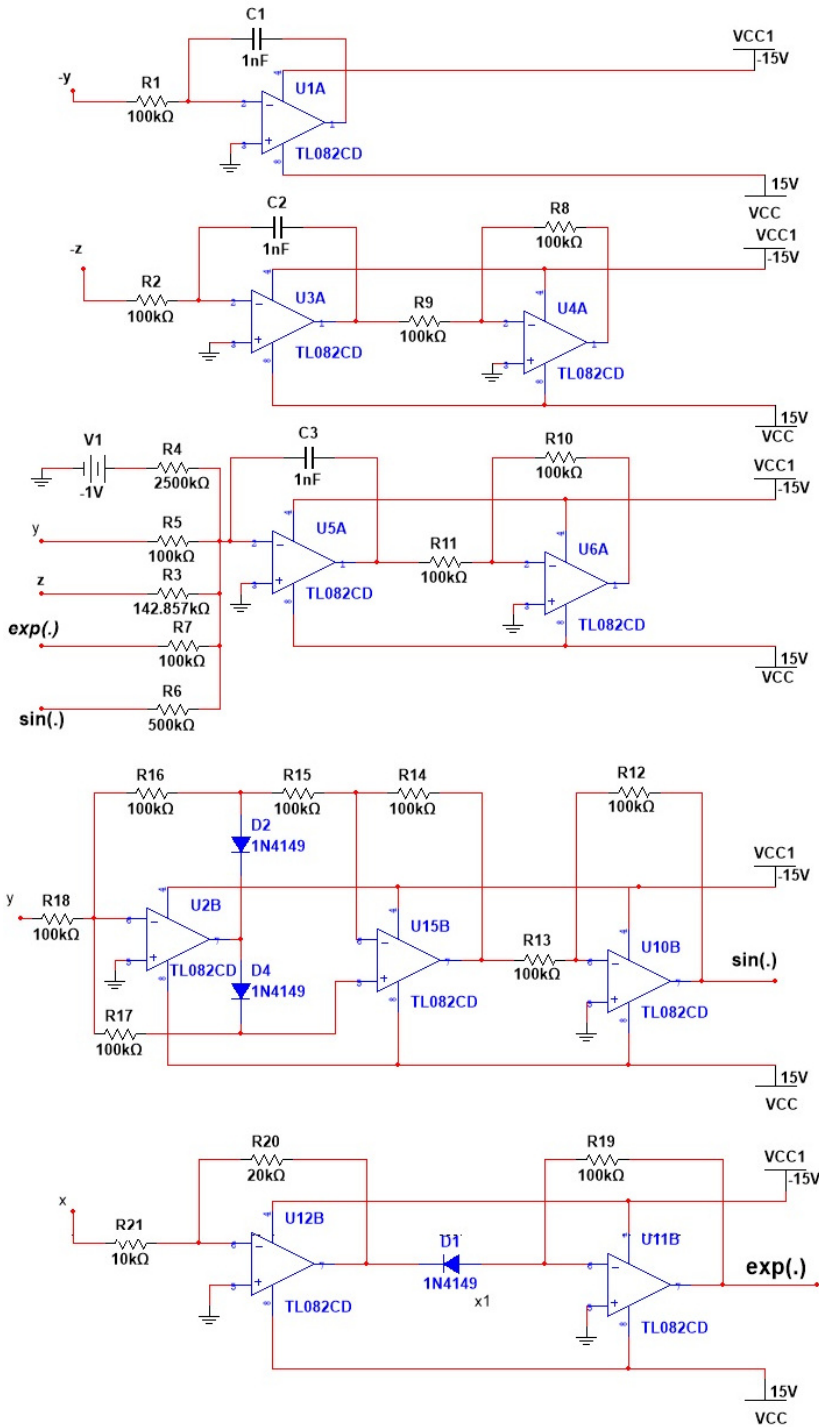


Figure 13: Circuit design of the new 3D modified WINDMI chaotic jerk system (7)

MultiSim 14.1 outputs of the jerk circuit (54) in different planes are presented in Figure 14. These results are consistent with the Matlab simulation results for the new modified WINDMI chaotic jerk system shown in Figure 1.

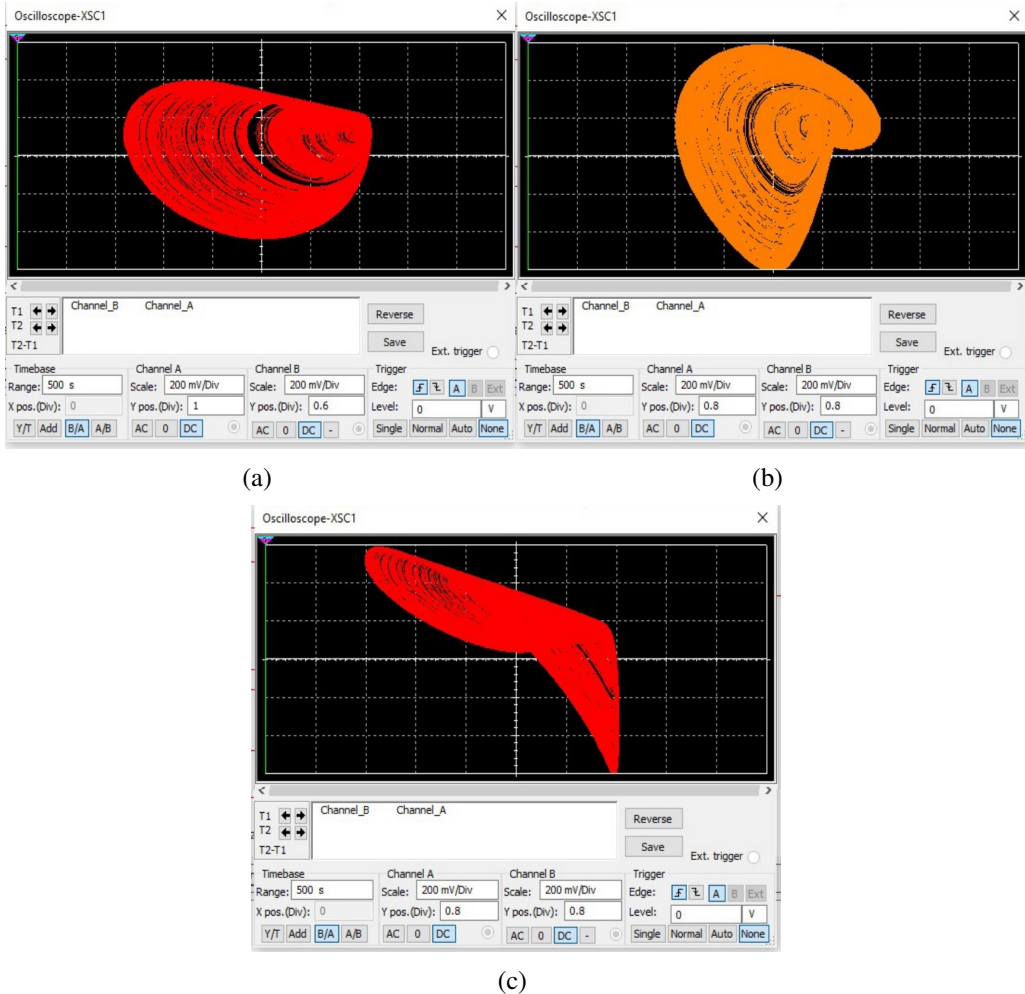


Figure 14: MultiSim 14.1 outputs showing the Chaotic attractor of the new 3D modified WINDMI jerk circuit (54) in different planes: (a) $(x - y)$ plane, (b) $(y - z)$ plane and (c) $(x - z)$ plane

6. Conclusion

This research work describes a novel new 3D modified WINDMI system with two nonlinearities. The proposed system is investigated using numerical mathematical tools namely; Lyapunov exponent spectrum, bifurcations diagrams,

0–1 test and Poincaré map. Also, we show that the new modified WINDMI system exhibit the propriety of co-existing of attractors. Finally, The physical existence of the chaotic attractor is verified by circuit realization of the novel modified WINDMI system using Multiim 14.1. The novel system and the obtained results of this work have many applications in many fields such as in secure communication and signal encryption.

References

- [1] P.-C. BÜRKNER, I. KOÖKER, S. OLADYSHKIN and W. NOWAK: A fully Bayesian sparse polynomial chaos expansion approach with joint priors on the coefficients and global selection of terms. *Journal of Computational Physics*, **488** (2023). DOI: [10.1016/j.jcp.2023.112210](https://doi.org/10.1016/j.jcp.2023.112210).
- [2] A. DE, A. NANDI, A. MALLICK, A.I. MIDDYA and S. ROY: Forecasting chaotic weather variables with echo state networks and a novel swing training approach. *Knowledge-Based Systems*, **269** (2023). DOI: [10.1016/j.knosys.2023.110506](https://doi.org/10.1016/j.knosys.2023.110506).
- [3] C. WANG and L. SONG: An image encryption scheme based on chaotic system and compressed sensing for multiple application scenarios. *Information Sciences*, **642** (2023). DOI: [10.1016/j.ins.2023.119166](https://doi.org/10.1016/j.ins.2023.119166).
- [4] X. LIU, X. TONG, Z. WANG, M. ZHANG and Y. FAN: A novel devaney chaotic map with uniform trajectory for color image encryption. *Applied Mathematical Modelling*, **120** (2023), 153–174. DOI: [10.1016/j.apm.2023.03.038](https://doi.org/10.1016/j.apm.2023.03.038).
- [5] Q. LAI and Y. LIU: A cross-channel color image encryption algorithm using two-dimensional hyperchaotic map. *Expert Systems with Applications*, **223** (2023). DOI: [10.1016/j.eswa.2023.119923](https://doi.org/10.1016/j.eswa.2023.119923).
- [6] H. JIA, J. LIU, W. LI and M. DU: A family of new generalized multi-scroll Hamiltonian conservative chaotic flows on invariant hypersurfaces and FPGA implementation. *Chaos, Solitons and Fractals*, **172** (2023). DOI: [10.1016/j.chaos.2023.113537](https://doi.org/10.1016/j.chaos.2023.113537).
- [7] Q. WAN, F. LI, J. LIU, S. CHEN and Z. YAN: A new memristive system with chaotic and periodic bursting and its FPGA implementation. *Circuits, Systems and Signal Processing*, **42**(1), (2023), 623–637. DOI: [10.1007/s00034-022-02136-x](https://doi.org/10.1007/s00034-022-02136-x).
- [8] Q. CHEN, B. LI, W. YIN, X. JIANG and X. CHEN: Bifurcation, chaos and fixed-time synchronization of memristor cellular neural networks. *Chaos, Solitons and Fractals*, **171** (2023). DOI: [10.1016/j.chaos.2023.113440](https://doi.org/10.1016/j.chaos.2023.113440).

- [9] Q. LAI and Z. CHEN: Grid-scroll memristive chaotic system with application to image encryption. *Chaos, Solitons and Fractals*, **170** (2023). DOI: [10.1016/j.chaos.2023.113341](https://doi.org/10.1016/j.chaos.2023.113341).
- [10] M. RAAB, J. ZEININGER, Y. SUCHORSKI, K. TOKUDA and G. RUPPRECHTER: Emergence of chaos in a compartmentalized catalytic reaction nanosystem. *Nature Communications*, **14**(1), (2023). DOI: [10.1038/s41467-023-36434-y](https://doi.org/10.1038/s41467-023-36434-y).
- [11] S. VAIDYANATHAN and A.T. AZAR: *Backstepping Control of Nonlinear Dynamical Systems*. Academic Press, Cambridge, USA, 2021.
- [12] F. LI and J. ZENG: Multi-scroll attractor and multi-stable dynamics of a three-dimensional jerk system. *Energies*, **16**(5), (2023). DOI: [10.3390/en16052494](https://doi.org/10.3390/en16052494).
- [13] E.D. DONGMO, J. RAMADOSS, A.R. TCHAMDA, M.E. SONE and K. RAJAGOPAL: FPGA implementation, controls and synchronization of autonomous Josephson junction jerk oscillator. *Physica Scripta*, **98**(3), (2023). DOI: [10.1088/1402-4896/acb85b](https://doi.org/10.1088/1402-4896/acb85b).
- [14] J. RAMADOSS, A.N. KENGNOU TELEM, J. KENGNE and K. RAJAGOPAL: Complex dynamics in a novel jerk system with septic nonlinearity: analysis, control, and circuit realization. *Physica Scripta*, **98**(1), (2022). DOI: [10.1088/1402-4896/aca449](https://doi.org/10.1088/1402-4896/aca449).
- [15] Q. LAI and C. LAI: Design and implementation of a new memristive chaotic system with coexisting attractors and offset boosting behaviors. *Indian Journal of Physics*, **96**(14), 4391–4401. DOI: [10.1007/s12648-022-02344-w](https://doi.org/10.1007/s12648-022-02344-w).
- [16] W. HORTON and I. DOXAS: A low-dimensional dynamical model for the solar wind the driven geotail-ionosphere system. *Journal of Geophysical Research: Space Physics*, **103**(A3) (1997), 4561–4572. DOI: [10.1029/97JA02417](https://doi.org/10.1029/97JA02417).
- [17] J.C. SPROTT: *Chaos and Time-Series Analysis*, Oxford University Press, New York, USA, 2003.
- [18] A. KUMAR and S. SINGH: Bifurcation analysis of a pulsating heat pipe. *International Journal of Thermal Sciences*, **192** (2023). DOI: [10.1016/j.ijthermalsci.2023.108384](https://doi.org/10.1016/j.ijthermalsci.2023.108384).
- [19] A. SINGH and V.S. SHARMA: Bifurcations and chaos control in a discrete-time prey–predator model with Holling type-II functional response and prey refuge. *Journal of Computational and Applied Mathematics*, **418** (2022). DOI: [10.1016/j.cam.2022.114666](https://doi.org/10.1016/j.cam.2022.114666).

- [20] A. SINGH and V.S. SHARMA: Codimension-2 bifurcation in a discrete predator-prey system with constant yield predator harvesting. *International Journal of Biomathematics*, **16**(5), (2023). DOI: [10.1142/S1793524522501091](https://doi.org/10.1142/S1793524522501091).
- [21] B.B.T. FRANCISCO and P.C. RECH: Multistability, period-adding, and spirals in a snap system with exponential nonlinearity. *European Physical Journal B*, **96**(5), (2023). DOI: [10.1140/epjb/s10051-023-00536-9](https://doi.org/10.1140/epjb/s10051-023-00536-9).
- [22] Z. ZHANG, L. HUANG, J. LIU, Q. GUO, C. YU and X. DU: Construction of a family of 5D Hamiltonian conservative hyperchaotic systems with multistability. *Physica A: Statistical Mechanics and Its Applications*, **620** (2023). DOI: [10.1016/j.physa.2023.128759](https://doi.org/10.1016/j.physa.2023.128759).
- [23] S. VAIDYANATHAN, A.T. AZAR, I.A. HAMEED, K. BENKOUIDER, E. TLELO-CUAUTLE, B. OVILLA-MARTINEZ, C.H. LIEN and A. SAMBAS: Bifurcation analysis, synchronization and FPGA implementation of a new 3-D jerk system with a stable equilibrium. *Mathematics*, **11**(12), (2023). DOI: [10.3390/math11122623](https://doi.org/10.3390/math11122623).
- [24] T. MA, J. MOU, A.A. AL-BARAKATI, H. JAHANSHAHI and S. LI: Coexistence behavior of a double-MR-based cellular neural network system and its circuit implementation. *Nonlinear Dynamics*, **111**(12), (2023), 11593–11611. DOI: [10.1007/s11071-023-08443-5](https://doi.org/10.1007/s11071-023-08443-5).
- [25] G. SIVAGANESH and K. SRINIVASAN: Theoretical investigations on the multistability, quasiperiodicity and synchronization of the driven Chua's circuit. *Circuits, Systems, and Signal Processing*, **42**(6), (2023), 3200–3228. DOI: [10.1007/s00034-022-02274-2](https://doi.org/10.1007/s00034-022-02274-2).
- [26] J. PETRZELA: Chaotic states of transistor-based tuned-collector oscillator. *Mathematics*, **11**(9), (2023). DOI: [10.3390/math11092213](https://doi.org/10.3390/math11092213).
- [27] K. ZOURMBA, C. FISCHER, B. GAMBO, J.Y. EFFA and A. MOHAMADOU: Chaotic oscillator with diode-inductor nonlinear bipole-based jerk circuit: Dynamical study and synchronization. *Journal of Circuits, Systems and Computers*, **32**(12), (2023). DOI: [10.1142/S0218126623502146](https://doi.org/10.1142/S0218126623502146).
- [28] F.E. ALSAADI, S. BEKIROS, Q. YAO, J. LIU and H. JAHANSHAHI: Achieving resilient chaos suppression and synchronization of fractional-order supply chains with fault-tolerant control. *Chaos, Solitons and Fractals*, **174** (2023). DOI: [10.1016/j.chaos.2023.113878](https://doi.org/10.1016/j.chaos.2023.113878).
- [29] H. CHENG, H. LI, Q. DAI and J. YANG: A deep reinforcement learning method to control chaos synchronization between two identical chaotic systems. *Chaos, Solitons and Fractals*, **174** (2023). DOI: [10.1016/j.chaos.2023.113809](https://doi.org/10.1016/j.chaos.2023.113809).

- [30] R. LUO, S. LIU, Z. SONG and F. ZHANG: Fixed-time control of a class of fractional-order chaotic systems via backstepping method. *Chaos, Solitons and Fractals*, **167** (2023). DOI: [10.1016/j.chaos.2022.113076](https://doi.org/10.1016/j.chaos.2022.113076).
- [31] S. YAN, J. WANG, E. WANG, Q. WANG, X. SUN and L. LI: A four-dimensional chaotic system with coexisting attractors and its backstepping control and synchronization. *Integration*, **91** (2023), 67–78. DOI: [10.1016/j.vlsi.2023.03.001](https://doi.org/10.1016/j.vlsi.2023.03.001).
- [32] N. DEBDOUCHE, L. ZAROUR, H. BENBOUHENNI, F. MEHAZZEM and B. DEF-FAF: Robust integral backstepping control microgrid connected photovoltaic System with battery energy storage through multi-functional voltage source inverter using direct power control SVM strategies. *Energy Reports*, **10** (2023), 565–580. DOI: [10.1016/j.egy.2023.07.012](https://doi.org/10.1016/j.egy.2023.07.012).
- [33] A. HOSSEINAJAD, N. MOHAJER and S. NAHAVANDI: Novel barrier Lyapunov function-based backstepping fault tolerant control system for an ROV with thruster constraints. *Ocean Engineering*, **285** (2023). DOI: [10.1016/j.oceaneng.2023.115312](https://doi.org/10.1016/j.oceaneng.2023.115312).